Brian Vohnsen, "The impact of aberrations in a 3D retinal model eye," Proc. SPIE 11814, Current Developments in Lens Design and Optical Engineering XXII, 1181405 (August 1, 2021).
DOI: https://doi.org/10.1117/12.2594117

The impact of aberrations in a 3D retinal model eye

B. Vohnsen*
Advanced Optical Imaging Group, School of Physics, University College Dublin, Dublin 4, Ireland

ABSTRACT

Aberrations of the eye degrade the ocular point-spread function thereby reducing the attainable visual acuity. It is common practice to distinguish between lower and higher-order monochromatic aberrations of the eye when differentiating between what can be corrected with sphere and cylinder, and what cannot. Nevertheless, at the retina it matters more whether light is incident along or obliquely onto the elongated photoreceptors. In this contribution, I discuss the impact of different Zernike aberration terms not at the pupil, but at the retina. Even-ordered monochromatic Zernike aberrations have an associated wavefront slope at the retina whereas odd-ordered Zernike aberration modes have no wavefront tilt across the point-spread function. In other words, even and odd-ordered Zernike modes are affected differently by the Stiles-Crawford effect of the first kind that relates to obliqueness of light at the retina. Understanding this is essential to decode how vision is triggered in normal viewing conditions as well as when probing vision and photoreceptors with psychophysical methods in the analysis of vision or for ophthalmic design. Finally, a uniaxial pupil flicker system is used to directly measure the integrated Stiles-Crawford effect in the author's eye in order to assess apodization of oblique light in normal vision.

Keywords: Stiles-Crawford effect, cone photoreceptors, aberrations, Zernike polynomials, point-spread function, visual acuity.

1. INTRODUCTION

Ocular aberrations degrade the point-spread function (PSF) causing a reduction in visual acuity. Monochromatic aberrations are commonly grouped as lower and higher-order aberrations to distinguish between those that can be easily corrected with sphere and cylinder and those that cannot.[1] Yet, even-ordered Zernike aberrations have an associated wavefront slope at the PSF whereas odd-ordered Zernike aberration modes are without wavefront tilt in the PSF. In consequence, even and odd-ordered Zernike aberrations of the eye are affected differently by the Stiles-Crawford effect of the first kind (SCE-I) that relates to obliqueness of light at the retina.[2-11] In this study, even and odd-ordered Zernike aberrations are studied individually with a simplified eye model to determine the impact of wavefront obliqueness in the retinal plane.

In the pupil plane the SCE-I is normally expressed by a Gaussian function as

$$\eta(r) = 10^{-\rho|r-r_0|^2} \tag{1}$$

where η is the effective visibility for a ray of light incident at point r. The function peaks at pupil point r_0 located near the pupil center. In foveal vision, the SCE-I directionality parameter is approximately $\rho \cong 0.05/\mathrm{mm}^2$. Yet, it is vital to recognize that the integrated SCE-I in normal viewing differs from the SCE-I determined with Maxwellian view. In normal vision through the natural pupil, direct numerical integration of Eq. (1) across the pupil is invalid. The truncation done by the SCE-I in normal viewing is nearly an order-of-magnitude higher than predicted by the directionality measured with Maxwellian view, although the match to a Gaussian function is not accurate. The integrated effective SCE-I visibility η_{int} for a pupil diameter d_{pupil} makes a better fit to a power law

$$\eta_{int}(d_{pupil}) = K \times d_{pupil}^{-m} \tag{2}$$

*brian.vohnsen@ucd.ie; phone +353 1716-2217; fax +353 1283-7275; https://www.ucd.ie/advancedopticalimaging/

where K is a scaling factor and m is a positive parameter.

We demonstrated this using a direct viewing pupil-size flicker system whereby the perceived brightness of light with a large pupil was matched to that of a small reference pupil.[6] The reason for this, is the 3D structure of the retina whereby light can leak from outer segments if obliquely incident on the retina.[5-9] Thus, the impact of aberrations should be evaluated in the retinal plane. Pupil apodization with a SCE-I is strictly valid only for the unaberrated eye as it cannot fully capture the impact of aberrations across the retina.[4]

We have explored this fact previously to cancel obliqueness of the wavefront in the retinal plane using annular apertures with coherent light that annul the Stiles-Crawford effect for oblique light.[10] In this case, the coherence of the light produces speckles in the retinal plane. Yet, the wavefront slope is zero below each speckle due to the symmetry of the illumination. We have also demonstrated that the same effect can be used to tune the wavefront slope at the retina with two opposing Maxwellian points in the pupil plane where an intensity difference is converted to wavefront slope at the retina thereby directly probing the traditional SCE-I directionality.[11] The importance of the local wavefront slope in the retinal plane is testimony to the role of the local direction of the energy flow across the retina.[12]

In this contribution, the impact of individual Zernike aberration terms is described in the retinal plane, rather than the pupil, in order to directly assess the obliqueness of light caused by aberrations at the retinal photoreceptors.[4] Leakage of light from the outer segments of photoreceptor cones is likely responsible for the SCE-I. Cones are packed in small groupings of similar cone types and thus leakage of light from one cone type, will leak into adjacent areas with other opsins causing the photopic directionality.[6,7,9] In turn, the lack of scotopic directionality is explained by the fact that peripheral rods are surrounded by more rods, and thus leaked light will potentially be captured by rhodopsin in adjacent rods thereby damping the angular sensitivity. The model is also used to describe the hue shift of the Stiles-Crawford effect of the second kind (SCE-II) that is observed after an accurate visibility match of the SCE-I.[13] Full knowledge of the SCE-I suffices to determine the SCE-II as the wavelength derivative of the SCE-I across a given bandwidth of the illumination.

This study finds that obliqueness of light at the retina is critical to decode how vision is triggered in normal viewing conditions as well as when probing vision and photoreceptors with psychophysical methods which matters in the analysis of vision and in ophthalmic design. The methodology is summarized in Section 2 which is followed by results and discussion in Section 3 and finally the conclusions in Section 4.

2. METHODOLOGY

Monochromatic lower and higher-order aberrations are commonly described at the pupil with Zernike polynomials as shown in Fig. 1. The impact on vision, is described by the PSF and its associated modulation transfer function (MTF). Yet, this process ignores the fact that photoreceptors are elongated and therefore impacted by obliqueness of light in the process of creating effective retinal images.[4] Fig. 2 shows the intensity PSF, and Fig. 3 shows the wavefront slope in the plane of the retina for the same PSF images.

The obliqueness of the wavefront at the retina is the cause of the SCE-I determined with Maxwellian light.[2-11] It also explains the presence of the SCE-II due to cross-coupling between adjacent but different cone types.

Apodization of the integrated SCE-I is significantly stronger in normal vision than with Maxwellian view.[6] We have previously analyzed effective visibility in normal vision through a flickering pupil. A motorized iris (Standa^{TM}) was set to flicker between a small 1.4 mm reference and a successively larger-and-larger test pupil. The brightness with a larger pupil was diminished by the observer using a liquid crystal tunable attenuator (Meadowlark^{TM}) so that a brightness match was obtained between the test and reference pupil sizes. The resulting effective visibility was matched to a traditional integration of the Gaussian SCE-I from Eq. (1), to a power law as in Eq. (2), and to an exponential function as

$$\eta_{int}(d_{pupil}) = \beta \times \exp\left(-\gamma d_{pupil}\right) \tag{3}$$

where γ is a positive coefficient and β is a scaling parameter. Finally, if aberrations are small, the traditional SCE-I function can be estimated from the measured integrated SCE-I function by means of a pupil-diameter derivative of the effective pupil area, or directly as

$$\eta_{estimate} = \frac{1}{2d_{pupil}} \times \frac{d}{dd_{pupil}} \left[\eta_{int} d_{pupil}^2\right] \quad (4)$$

which would lead to Eq. (1) if the traditional SCE-I function could be integrated across the pupil.

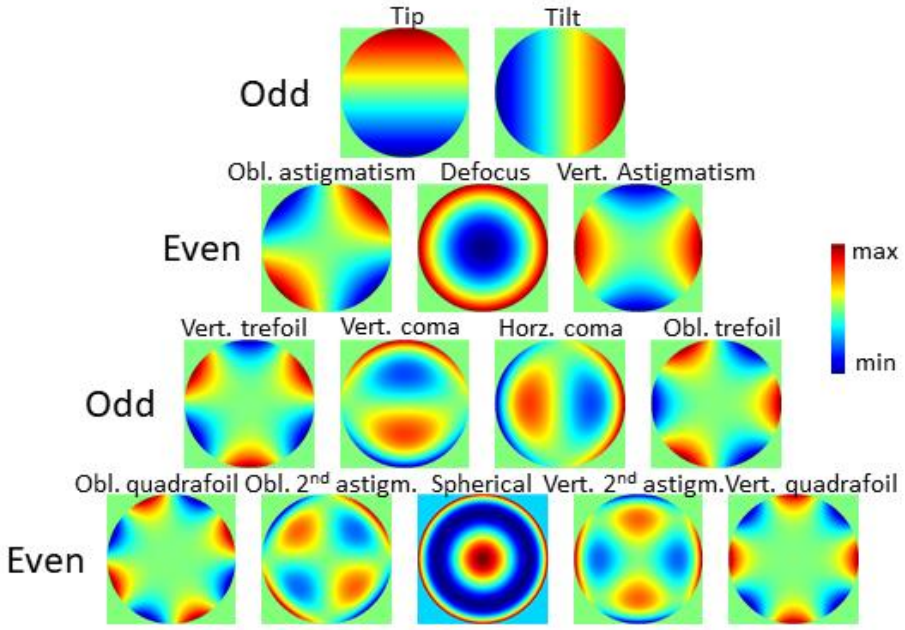

Figure 1. Wavefront representation of Zernike polynomials in the pupil plane. Each coefficient has been set to 1µm.

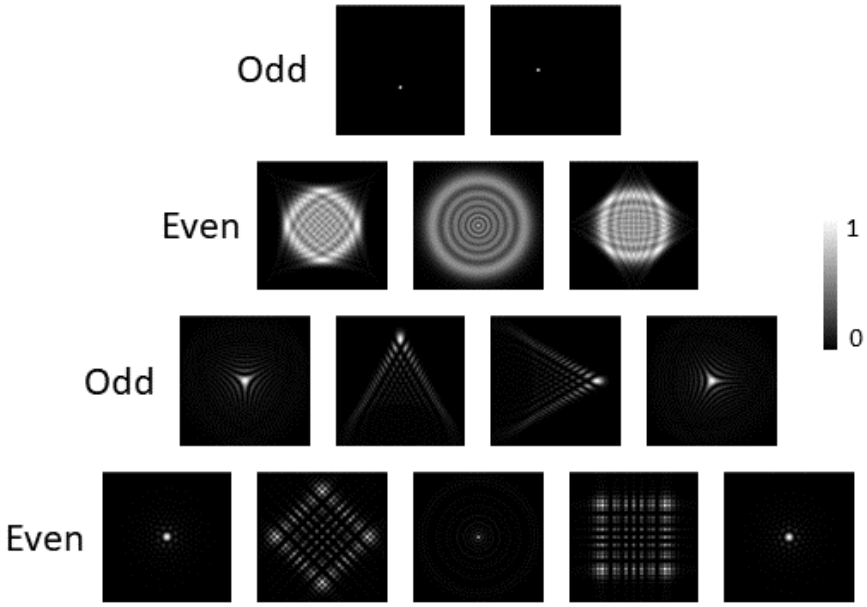

Figure 2. Normalized intensity PSF's of individual Zernike aberrations in the retinal plane using a schematic eye model with axial length f_{eye} = 22.2 mm, effective refractive index n_{eye} = 1.33 and d_{pupil} = 5 mm.[3,4] Each image is 50 µm × 50 µm.

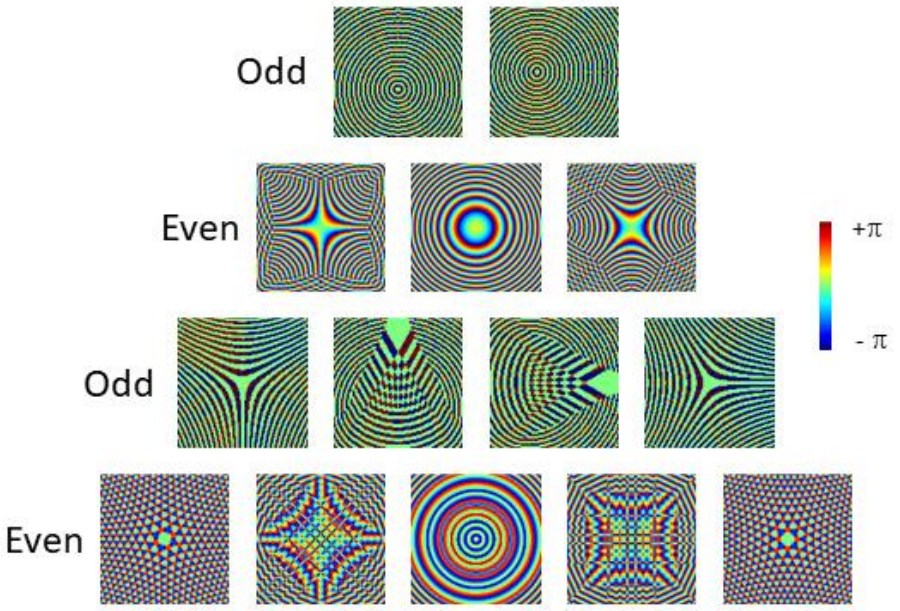

Figure 3. Accompanying wavefront slope of each PSF shown in Fig. 2 in the retinal plane, wrapped onto [-π;π[. As seen, only even-order Zernike polynomials have a tilted wavefront slope in the retinal plane, whereas odd-order polynomials have sign reversals of the field amplitude. As before, f_{eye} = 22.2 mm, n_{eye} = 1.33 and d_{pupil} = 5 mm. Each image is 50 µm × 50 µm.

3. RESULTS AND DISCUSSION

The wavefront of the PSF's in the retinal plane associated with different Zernike polynomials in Fig. 3 shows that only even radial orders have an associated wavefront tilt. Thus, they will be attenuated by the SCE-I whereas the odd radial orders will not.[4] Describing the aberrations directly in the retinal plane where vision is triggered is therefore fundamentally more appealing than in the pupil plane. This gives optical insight into why the eye is best adapted to its own aberrations[14] without relying on neural cues. It also makes it clear, that it needs careful consideration of the integrated SCE-I in optical design.[15]

Measurements of the integrated SCE-I for the author's own right eye dilated with tropicamide are shown in Fig. 4 using the pupil flicker system at three different wavelengths. Each pupil size is repeatedly present for 1 sec. (reference and test pupil size flicker) until a satisfactory brightness match has been achieved by dimming the larger pupil, at which point a measurement is taken and the test pupil moves to a successively larger diameter. The methodology is described in detail in Ref. (6).

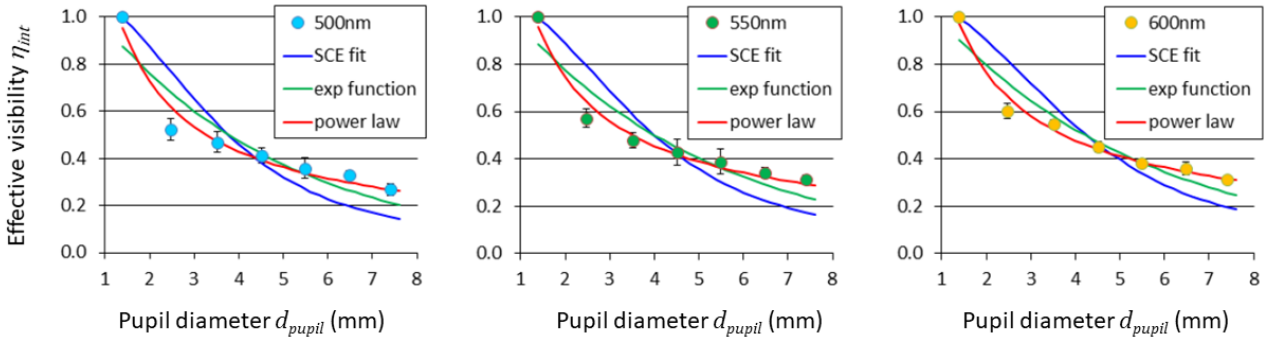

Figure 4. Effective visibility curves at three wavelengths determined in the right eye of the author with 4 repetitions (error bars show the standard deviation). The measured data have been fitted to the integral of the Gaussian SCE-I function (blue line), the exponential function in Eq. (3) (green line), and the power law in Eq. (2) (red line).

The results prove that the integrated SCE-I has a strong apodization effect for small pupil sizes. The effect is best fitted to a power law as expressed in Eq. (2). This can also be appreciated from the fitting data summarized in Table 1. In other words, the gentle truncation expressed by the Gaussian SCE-I function in Eq. (1) is not representative for vision through the natural pupil.

Table 1. The quality of the fitting functions used for the integrated SCE-I measurements for the author's right eye and the data shown in Fig. 4. The fits are based on the optimized Levenberg-Marquardt method and the quality of each fit is expressed by its R-squared value.

Wavelength	**500 nm**	**550 nm**	**600 nm**
Gaussian SCE-I	ρ = 0.238/mm^2 (R-squared: 0.70)	ρ = 0.206/mm^2 (R-squared: 0.70)	ρ = 0.179/mm^2 (R-squared: 0.76)
Exponential function	β = 1.222; γ = 0.237 (R-squared: 0.86)	β = 1.202; γ = 0.219 (R-squared: 0.87)	β = 1.212; γ = 0.209 (R-squared: 0.91)
Power law	K = 1.233; m = 0.762 (R-squared: 0.97)	K = 1.220; m = 0.711 (R-squared: 0.98)	K = 1.221; m = 0.676 (R-squared: 0.99)

4. CONCLUSIONS

The present study builds on an earlier study by the author on the impact of wavefront aberrations at the retina[4] but goes further in the analysis of data obtained with the pupil-size flickering system to directly determine a best fitting function for the integrated SCE-I in normal vision.[6] It shows a power law for the reduction in visibility with increasing pupil size that strongly attenuates oblique light rays as produced by either a large pupil or even-order Zernike aberrations (defocus, astigmatism, spherical aberration, etc.). The distinction between even and odd radial Zernike orders in terms of wavefront tilt at the PSF in the retinal plane shows an important role of the integrated SCE-I that directly impacts on vision but that is commonly overlooked when assuming a Gaussian SCE-I apodization at the pupil plane.

ACKNOWLEDGMENTS

The author is grateful to Dr. Benjamin Lochocki, Dr. Alessandra Carmichael Martins, Dr. Najnin Sharmin, Dr. Salihah Qaysi, and Dr. Denise Valente who all assisted with measurements in the flickering system used to directly measure the visual impact of the integrated SCE-I.

REFERENCES

[1] Thibos, L. N., Hong, X., Bradley, A., and Cheng, X., "Statistical variation of aberration structure and image quality in a normal population of healthy eyes," J. Opt. Soc. Am. A 19(12) 2329–2348 (2002).
[2] Stiles, W. S. and Crawford, B. H., "The luminous efficiency of rays entering the eye pupil at different points," Proc. R. Soc. London 112, 428–450 (1933).
[3] Vohnsen, B., Iglesias, I., and Artal, P., "Guided light and diffraction model of human-eye photoreceptors," J. Opt. Soc. Am. A 22(11), 2318–2328 (2005).
[4] Vohnsen, B., "Photoreceptor waveguides and effective retinal image quality," J. Opt. Soc. Am. A 24(3), 597–607 (2007).
[5] Vohnsen, B., "Directional sensitivity of the retina: A layered scattering model of outer-segment photoreceptor pigments," Biomed. Opt. Express 5(5), 1569–1587 (2014).
[6] Vohnsen, B., Carmichael, A., Sharmin, N., Qaysi, S. and Valente, D., "Volumetric integration model of the Stiles-Crawford effect of the first kind and its experimental verification," J. Vision 17(12):18, 1–11 (2017).
[7] Carmichael Martins, A. and Vohnsen, B., "Directional light-capture efficiency of the foveal and parafoveal photoreceptors at different luminance levels: an experimental and analytical study," Biomed. Opt. Express 10(8), 3760–3772 (2019).
[8] Meadway, A. and Sincich, L. C., "Light propagation and capture in cone photoreceptors," Biomed. Opt. Express 9(11), 5543–5565 (2018).
[9] Nilagiri, V. N., Suheimat, M., Lambert, A. J., Turpin, A., Vohnsen, B. and Atchison, D. A., "Subjective measurement of the Stiles-Crawford effect with different field sizes," Biomed. Opt. Express 12(8), 4969–4981 (2021).
[10] Vohnsen, B. and Rativa, D., "Absence of an integrated Stiles–Crawford function for coherent light," J. Vision 11(1), 19 (2011).
[11] Castillo, S. and Vohnsen, B., "Exploring the Stiles–Crawford effect of the first kind with coherent light and dual Maxwellian sources," Applied Optics 52 (1), A1–A8 (2013).
[12] Westheimer, G., "Retinal light distributions, the Stiles–Crawford effect and apodization," J. Opt. Soc. Am. A 30, 1417–421 (2013).
[13] Vohnsen, B., "On the spectral relation between the first and second Stiles-Crawford effect," J. Mod. Opt. 56(20), 2261–2271 (2009).
[14] Artal, P., Chen. L., Fernández, E. J., Singer, B., Manzanera, S. and Williams, D. R., "Neural compensation for the eye's optical aberrations," J. Vision 16(4), 281–287 (2004).
[15] Norrby, S., Piers, P., Campbell, C., and van der Mooren, M., "Model eyes for evaluation of intraocular lenses," Appl. Opt. 46(26), 6595–6605 (2007).